International Journal of Sciences: Basic and Applied Research (IJSBAR)

ISSN 2307-4531
(Print & Online)

http://gssrr.org/index.php?journal=JournalOfBasicAndApplied

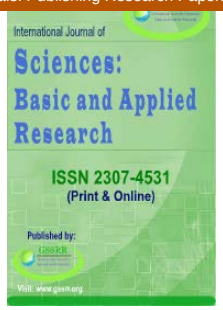

Yinchuan City within Northwest China - GROUND-Based Remote Sensing Aerosol Optical Properties

Ferdinand Shimei[a*], Okeke F. N.[b], Akujor C. E.[c], Chineke T. C.[d], Nwofor O. K.[f]

[a,b,c,d,f] *Department of Physics and Industrial Physics, Imo State University, P.M.B 2000 Owerri, Nigeria*

Email: jehos_haphat@yahoo.com

Abstract

A ground-based sky radiometer was used to evaluate straight and scattering solar irradiances, as well as aureole radiances, from October 2003 to August 2004 within Yinchuan in China. Aerosol particles optical depth AOD, Angstrom exponent (ALPHA), degree size circulation, refraction index and distinct scattering albedo of aerosols were simultaneously reclaimed by means of the 'SKYRAD' cryptogram. The results disclosed that throughout the study period, the AOD diverse periodically, with a vernal utmost and a winter minimum, and the distinction in ALPHA was totally different, with a vernal least and a winter utmost. The diurnal inconsistency of AOD was momentous, demonstrated a similar distinction pattern in spring, summer and autumn and had another distinction pattern in winter. The frequency circulation of AOD and ALPHA roughly follow a log-normal likelihood circulation and a normal likelihood circulation, respectively. The correlation between ALPHA and AOD illustrated a simple dependence of ALPHA on AOD in spring and can be distinguish by one incorporate exponential function. And no clear association between AOD and ALPHA was obvious in other seasons. The aerosol degree size distributions can be typify by the sum of two log-normal circulations, and symbolized an accretion mode with a radius of approximately 0.16 μm, and a loutish mode with a radius of approximately 8 μm, which was the major aerosol mode in this area. The real fractions of the refraction catalog rose in spring, and demonstrated a low understanding to wavelengths; the unreal parts of the refractive index reduced noticeably in spring and also demonstrated a low understanding to wavelength. Equally their low sensitivities to wavelengths are little different with time, but no comprehensible patterns were found.

---

* Corresponding author.

The aerosol lone scattering albedo in spring was greatly higher than in other season and improved spectacularly with increase in wavelength, from 0.93 at 400 nm to 0.98 at 1020 nm. In other seasons, it demonstrated a faintly reduced with wavelength. The aerosol straight radiative forcing effectiveness at the short wavelength is - 55.32, - 59.72, -60.14 and -60.39 at surface and 13.90, 10.40, 2.31 and 2.65 at TOA in spring, summer, autumn and winter, in that-order. The importance at surface; TOA in spring is lower/higher than that in other period, signifying the control of the dust aerosol.

Keywords: Yinchuan-Aerosol; Optical properties; Sky- radiometer; Radiative forcing.

1. Introduction

Aerosols consist of one vital component of the Earth atmosphere structure, which control radiative transfer in the atmosphere and take part in a tremendously significant role both in universal climatic change and in the biogeochemical cycle. Numerous studies concerning the retrieval of aerosol particles optical properties, their disposition of spatial and sequential variations, and their control on atmospheric radiation and climate have been carried out [1,2,3,4,5,6,7,8,9]. Though, these aerosol consequences still contain substantial uncertainties due to the poor perceptive of aerosol properties and their spatial and sequential variation and aerosol maintain to play a fundamental role in contemporary evaluations and forecasts of global climate [10].

Ground-based remote sensing of aerosols is perfect for the dependably and incessantly derivation of aerosol particles properties in key sites around the world and further information than can be acquired from space-borne remote sensing, with no surroundings signal ground-based AOD nevertheless is more dependable. It always delivers efficient standards, representative for the entire perpendicular column with no height reliance and is mainly true for the refractive indices and the size circulation parameters of the particle size distribution in authenticating aerosol product acquired from different satellite sensors could need ground-based measurements of a diversity of optical aerosol distinctiveness with diverse data excellence requirements.

1.1 Definition of Problem

To understand many aerosol ground-based observation networks that has been established in order to understand the optical properties. To indirectly evaluate their effect on climate, including AERONET; An Automatic Robotic Sun and Sky Scanning Measurement Program [11], SKYNET A Sun and Sky Radiometer Network Based in East-Asia [12], and GAW (Global Atmosphere Watch Programme) [13].

It is well implicit that aerosols are not well-mixed in the atmosphere so aerosol particles properties, such as the optical depth (AOD), the Angstrom exponent (ALPHA) and others would depend on site circumstances that govern emission, transport, atmospheric renovation and elimination of aerosol particles. Given the diminutive lifetime of aerosol particles, their properties differ with time and from one area to another. Yinchuan geographical location Latitude: 38°28′05″N, Longitude: 106°16′23″E; Elevation above sea level: 1117 m = 3664 ft is located at the northwest of Ningxia province of China, which is a distinctive semiarid area near by desert and Gobi. The yearly average rainfall there is about 200 mm and the yearly average of temperature is 8.5°C with enormous yearly and daily variations. The monthly average of wind speed is approximately 2 m/s, with huge

standards occurred in spring. So, it is recurrently affected by dust storms, particularly in spring. Although, due to the influence of the mountain, situated at west of it, the effects of dust are less grave than that in several other locations in northwest China, such as Dunhuang locations.

Furthermore, majority cities in north China, however is also a city with soaring industrial pollution. So the aerosol particles properties over this region are good representative for the most areas in northwest China. Owing to its extraordinary site and good infrastructure, however, Yinchuan has been recognized as one of the best locations for many international aerosol field researches, such as, China and Japan joint plan on Aeolian dust effect on climate (ADEC).

1.2. The Objective of this Study

The purpose of this study is to identify and quantify at the same time reclaim aerosol particles optical depth, Angstrom exponent, size circulation, single scattering albedo, as well as the real valid and unreal parts of the refractive index over Yinchuan region during using of straight and scattering solar irradiances, as sound as aureole radiances the area of improved brightness that background the solar disk in cloudless situation and is mostly owed to the advance single scattering of light by the aerosol particles from an atmosphere radiometer. The outcome of this research will give us an insight on the level and classification of the climatology of these aerosol particles optical properties conversed and the aerosol straight radiative effects are also predictable, which will break to improve contemporary knowledge about aerosols in this region and within the world.

1.3. Significance of the Study

This study provides insight to the ground-based remote sensing aerosol optical properties within Yinchuan in northwest china city. Create public awareness and information to evaluate the direct scattering solar irradiances, as well as aureole radiances, from October 2003 to August 2004 over Yinchuan, China. Understand the very important consequences of anthropogenic and natural pollutants hauling on the physical and optical properties of area milieu atmospheric aerosol.

1.4. Limitation of Study

Hitherto, we have merely fractional perceptive of the information intellectually interesting material and accuracy of the radiative relocate inversion of aerosol information via satellite data, due to lack of adequate theoretical analysis and relevance to apposite field data. This limitation will create the expected new data even further interesting and challenging. The foremost worry is the present insufficient aptitude to sense aerosol absorption, through space or from the ground. Absorption is a decisive parameter for climate investigation and atmospheric corrections. Prospective development in aerosol retrieval and atmospheric corrections may necessitate improved climatology of the aerosol properties and mutual comprehension of the effects of assorted composition and shape of the particles. The major constituents absent in the designed remote sensing of aerosol are space~borne and ground~based lidar observations of the aerosol silhouette. This article thrashed out the functioning state and thinking of the monitoring system, the precision with accuracy of the measuring radiometers, a succinct elucidation of the processing system, and entrance to the database.

2. Data and Instrumentation

2.1. Data

The first thing is direct and scattering solar irradiance measurements, and aureole radiance measurements, were taken at the Yinchuan observation location Latitude: 106.21°E; Longitude: 38.48°N; Altitude: 1111m). Next the sampling hiatus is 11 min from sun rises to sun sets beneath clear skies. The observation epoch was from October 2003-August 2004. Owing to the breakdown of radiometer, the data of September were missed. Plane stresses wanted for Rayleigh scattering optical depth computation were acquired through the Yinchuan meteorological observatory situated near the observation station. However, the columnar ozone contents for ozone absorption optical depth computations were acquired from the Total Ozone Mapping Spectrometer. Surface albedos over Yinchuan region were obtained from the MODIS outer surface albedo results.

2.2. Equipment and standardization

The ground-based sky radiometer POM-0 1; is a product of Prede Co., Ltd., Tokyo, Japan is a suitable, portable instrument that can calculate direct and scattering solar irradiances, also the aureole in the solar almucantar and the major plane, in daytime under lucid skies. It consists of seven filters with the innermost wavelengths from 315, 400, 500, 675, 870, 940, and 1020nm; the half bandwidth wavelength at 315 nm is 4 nm and less than 11 nm at the other wavelengths. Measurements made at 315 and 940 nm are used for deriving the O_3 attentiveness and rainfall water column quantity, respectively; measurements at the further wavelengths are used for aerosol remote sensing. The field of sight is 1° and the least angle for sky measurements is about 4^o, the photometer is mounted on a vertical/horizontal two axis mount that is determined by digital servomotors to carry out sky radiance almucantar measurements. An advance programmed sequence of measurements is taken by the aureolemeter: throughout epoch when the air mass is larger than 4 , solar direct and scattering measurements are made approximately 0.26 air mass intermission, while at lesser air masses, the example interval is typically 11 mm. information of the scanning system can be found in [14].

Precise standardize of the radiometer constant, $X_{0,}\lambda$ is important in ground-based measurements [15]. The precision with which AOD can be retrieved depends mostly on the precision of the $X_{0,}\lambda$, worth. X0,λ while errors should be less than 3% in order to acquire AOD with an doubt less than 0.03 while the air mass is equivalent to 1. The Langley method (LM), an uncomplicated application of the Bouguer Lamber Beer law, is basically the de facto typical, due to its high precision and its expedient relevance in the field. The hypothesis that the atmosphere stay steady throughout the standardization epoch of one to numerous hours is not contented at most sites and under mainly circumstances. Consequently, some modified Langley methods (MLMs) have been urbanized in which provisionally capricious atmospheric turbidity is taken into deliberation [16]. This paper, the radiometer was standardized using the modified Langley method recommended by [17], which is an expansion of the Tanaka's MLM. The first rung entails performing an reversal with merely further scattering intensity data (3^o- 41^o), form which momentarily capricious aerosol optical depth (AOD) are obtained. There are two motives for only in view of the further scattering. One explanation is that the further scattering part (3^o-41°) is mostly made up of diffracted radiation which is typically reliant on the scattering traverse section of particles

lacking a great deal reliance on the refractive index particularly feasibly index and non~sphericity. Furthermore is that this fraction is just circum~solar area which likely not to be pretentious by inhomogeneity of the level aerosol distribution and ozone absorption and so on. These AOD standards are then proliferated by the matching air mass (m) and used to acquire the radiometer constant In(ϕ0) in the course of the Beer Lambert's equation: In(ϕ) = In(ϕ0) - m AOD. In this development, AOD can be a bumpy approximate of atmospheric turbidity which comprises the brief revolutionize through the Langley plot. And this system is not pretentious by such temporal revolutionize of AOD by means of an AOD with a brief change incorporated, even if it is a bumpy approximation. A thoughtful study illustrated that the results of the uncertainties in the input stricture, such as refractive index, and measurement errors on standardization were weak, so a standardization accuracy of 2% can be attained by this system. Therefore, the errors in AOD retrievals are roughly 0.02 at one air mass.

3. Methodology

Aerosol properties were repossessed with the latest edition (v4.2, April 2006) of the 'SKYRAD' code, which was urbanized by [17]. The cipher comprises two programs: the first is for calculating replicated direct and diffuse solar radiation, which is for building a test simulation data for the inversion cipher and revisits the replicated spectral angular circulation of sky radiance and straight solar irradiance into the capricious AUR for every angle 0 signify direct and wavelength. The second is meant for reclaim aerosol properties from solar radiation data authentic or replicated. In this code, the input data mostly consist of the solar zenith angle and geometry almucantar, primary plane, the numeral and significance of wavelengths and scattering angles, the standardized radiometer stable of radiometer the surface stresses, the ozone content, the surface albedos, latitude, longitude and altitude beyond observation site, the smallest and utmost radii of aerosol particles, and the unspoken refractive index for every wavelength [17]. Next the aerosol optical depth, size circulation, single scattering albedo and refractive index can be repossess from the observation of straight and scattering solar irradiances, as well as aureole radiances. Its formation and inversion precision are discussed in detail in the literature [17,18]. And on an average, the errors for the smallest and utmost size ranges (0.06-0.1μm and 7-16μm) may be as large as 36-100%, but the accuracy for the middle range is anticipated to be bigger than 81%.

The Angstrom exponent is resolute from the spectral reliance of the calculated optical depth, and is a good meter of the aerosol size. The coefficient is calculated using the regression analysis, in which the AOD values for three wavelengths (400, 500 and 675 nm) are fitted to the subsequent equation:

$$\tau\rho\ (\lambda) = \varphi\lambda^{-\text{alpha}} \qquad (1).$$

Where λ is the wavelength and φ is the aerosol turbidity and the coefficient (AOD) at λ = 1μm). The data for ALPHA are used only when an excellent correlation coefficient R>0.91 is acquired in the regression analysis by means of Equation (1).

The radiometer automatically gathered data regarding of sky circumstances excluding for rainy circumstances according to a preprogrammed progression, therefore, the cloud screening is important for data excellence function. Here, the cloud screening system established by [19] and practical to AERONET data was exploiting.

This method is foundation on the principle that clouds have huge optical depths and larger temporal inconsistency than do aerosols. Furthermore, physical cloud screening for problematic data was carried out using weather observations from the Yinchuan observatory.

The aerosol radiative forcing (ARF) at the peak of the atmosphere (TOA) and at the surface is explained as the distinction in the net fluxes losing minus upbeat solar bonus long wave; in W m2 with and lacking aerosol at the TOA and at the surface levels, in that order. The aerosol straight radiative forcing effectiveness is explained as the ratio amid the ARF significance and its parallel AOD value [20]. To transmit out the radiative forcing calculations we used the Santa Barbara DISORT Atmospheric Radiative Transfer (SB-DART) model [21], which is urbanized by the atmospheric science district, and is a distinct ordinates radiative transfer model [22]. It is being used extensively for the radiative transfer computations, this algorithm comprises multiple scattering in a perpendicularly inhomogeneous non isothermal plane parallel media, also, and it has been demonstrate to be computationally resourceful and to dependably resolve the radiative transfer equation. The major input data consists of the solar apex angle, where you have the view of stipulated a particular solar zenith angle or enter a particular date, time, latitude and longitude to compute the solar zenith angle with one small code in the SB-DART; the spectrum range of computing fluxes, where you can select the shortwave 0.25-4.1µm, long wave 4.0-101µm and entire spectrum 0.25-101µm; atmospheric silhouette nine standard; the trace gases including CO_2,CH_4 and N_2O the default standards or any input standards; the surface albedo model six diverse surfaces you can select or input your own value; the aerosol stricture, where you can choose no aerosols or one particular aerosol replica from four replicas and input the AOD551 nm; the cloud stricture and the stricture what you want to achieve. The output data for each sprint consist of down flux, up flux, direct flux and net flux for the entire atmospheric column or down flux, up flux, direct flux at which spot in the atmospheric column “top or bottom” for the ten capricious, plus hour of day, solar apex angle, wavelength, ect at the given range and step. The generally uncertainty in the anticipated forcing due to divergence in imitation is found in the range 10-16%. And the comprehensive conversation about this model is in the literature [21]. In our study, we computed the down radiative flux and up radiative flux at the surface and TOA for the erratic wavelength Variety from 0.26µm to 4.1µm with a step of 0.26µm, beneath the aerosol current and not. Then the radiative forcing effectiveness was projected at the surface and TOA at the 0.25-5 µm. The solar zenith angles have used the periodic average value. And support upon the geographical site, calculated stricture and the widespread weather circumstances, we have used the midlatitude summer atmospheric outline for spring, summer and autumn and the midlatitude winter atmospheric outline for winter, and have used the default importance of trace gases and the urban aerosol model. The AOD551 nm value is gritty from the value of AOD500 nm using the power law as follows:

AOD551 AOD500 nm 551/500 alpha where alpha is the Angstrom exponent 400-675 nm [23].

4. Results and Discussion

4.1. Angstrom Exponent with Aerosol Optical Depth (AOD)

The AOD is ambassador of the airborne aerosol stack in the atmospheric column and is imperative for the recognition of aerosol source area and aerosol evolution. Here Figure1 illustrates the monthly mean aerosol

optical depth at 500 nm from October 2003 to August 2004, with error bars illustrating the normal deviation of the monthly averaged value. The mean AOD differ on a monthly foundation with the negligible standards happening from October-February with a least in February 0.176+0.020, demonstrating that the atmosphere was comparatively clean throughout this period. Due to the data of Chinese dust storm net http://wwwduststrorn.com.cn, there were entirety fourteen dust incidents in 2004, and majority of those occurred in spring. Owing to the pressure of these dust actions, the AOD enlarged from March-May, getting its maximum worth in May 0.399+0.029. The mean

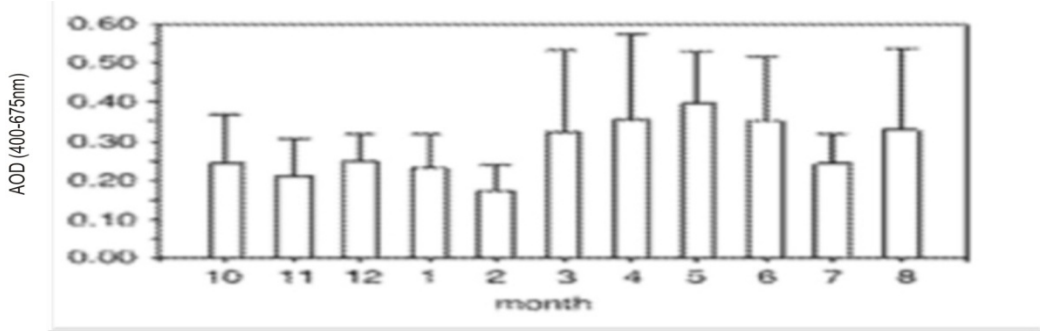

Figure1: Monthly average aerosol optical depth 500nm and standard deviation (courtesy Atmos)

AOD in June and August was a little lesser than that in May, though was also elevated, reflecting the control of inhabitant atmospheric dust particles after dust actions in June and local meteorological circumstances, like high temperature, and pollutant particles in August [24]. The relatively lesser mean AOD in July owed to wash-out by rainfall actions. Usually, the AOD standards were lesser in fall and winter and larger in spring and summer, [25] established that AOD standards were lesser in summer and fall and larger in winter and spring, based on spectrophotometer data collected at Yinchuan in 2002. This demonstrated how AOD can differ over time and is influenced by climatic circumstances. Figure.2 is the monthly mean ALPHA 400- 675 nm, and its standard deviation. On the entire, the change in ALPHA was opposed to that of AOD. The minimum ALPHA values emerged in March to May, which shows that the aerosol particles were huge through this period and likely associated to dust actions. Smaller aerosol particles emerge to control during November to January including July. Furthermore, ALPHA and AOD standards were high in August, which points out that there was an increase in the donation of fine particles throughout this high temperature period [26]. ALPHA standards were always bigger than 0.6 except during

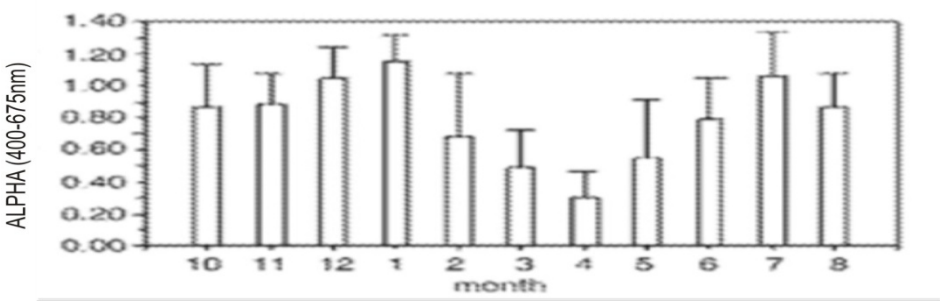

Figure 2: Monthly average Angstrom exponent 400-675 nm and standard deviation (courtesyAtmos)

March and April, this shows the bigger contribution of fine particles to annihilation over the Yinchuan area.

Diurnal changeability of aerosol optical depth is imperative for different applications, as well as satellite aerosol data substantiation, radiative forcing calculations, studies of aerosol relations with humidity and clouds, like wise public health [26,27]. Mainly urban industrial AERONET locations, a widespread pattern of the AOD was indicated to increase by 10-41% throughout the daytime and the dust aerosol could not be comprehensive a diurnal tendency [27]. Figure 3 illustrates the diurnal inconsistency of aerosol optical depth at a wavelength 500nm. All entity observations for a day are articulated as a percentage exodus from the daily mean. Calculated percentages were averaged hourly 0301-0401 GMT, 0401-0501 GMT etc. for every measurement epoch. The sampling process which is comparable to one used by [28], makes a systematic diurnal tendency more evident. The diurnal inconsistency of AOD in Yinchuan was momentous, and its assortment about 32%, 34%, 25% and 39% in spring, summer, autumn and winter, respectively. AOD progressively increased in the morning, reaching the utmost worth and then lessened spectacularly in spring, summer and autumn, and the only distinction was the time of utmost in each season. However, in winter, AOD increased first, reaching the maximum at 13:01 pm and after that decreased, however increased again from 15:01pm. [29,30] established that the AOD progressively increased all through the daytime and attained maximum in the late afternoon for mainly urban and industrial regions, inclusive Beijing, situated in north of China. This distinction is mostly due to the dissimilar composing of aerosol and climatic circumstances.

Several studies have sported that the precise statistic description of AOD can precisely search for one apposite parameterization which is as simple as probable although attaining a level of circulation

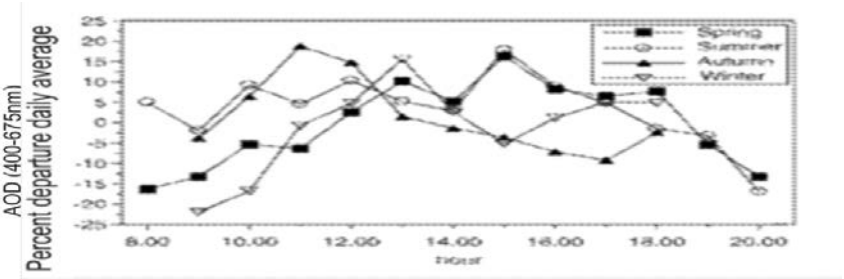

Figure 3: Diurnal variability of AOD calculated hourly as percent exodus from daily average. (courtesy Atmos)

Characterization which contents to the precision wants of model compelled applications such as radiative forcing or aerosol scattering, like wise tell us something further about the distinction of natural phenomena [31]. Earlier studies have revealed that the frequency circulation of AOD, τ, can be illustrated by the subsequent log-normal circulation:

$$\delta(\tau) = \frac{1}{s\tau\sqrt{2\pi}} \exp\left(\frac{(\ln\tau - m)^2}{2s^2}\right)$$

this means that 1nδ go after a Gaussian or usual circulation with mean, m, and the standard deviation, s [31][32][33][34]. Figsure4 and figure5 illustrates the frequency distributions of AOD 500nm and ALPHA 400-675 nm for every season. Excluding from the data of influenced by cloud, the digit statistics of samples is 1293, 1487, 1444 and 1493 in spring, summer, autumn and winter respectively.

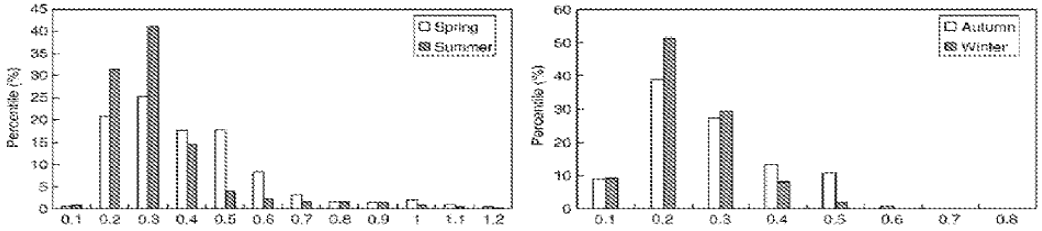

Figure 4: The frequency distributions AOT 500nm for each season in Yinchuan left; spring and summer; right; autumn and winter (courtesy Atmos)

Founded on results from spring and summer, it is further appropriate to show AOD frequency circulations by the log-usual probability circulation than by a usual probability distribution, which is unfailing with [31]. The usual probability circulation was establish to better symbolize ALPHA frequency distributions [31][35], particularly in summer in our study. Figure 4 demonstrated that roughly 82% of the AODs arrayed amid 0.1 and 0.6 and that 56% of the AODs arrayed between 0.4 and 0.6 in spring; about 73%, 67% and 80.9% varied between 0.1 and 0.4 in summer, autumn and winter, in that order. Particularly in winter, nearly 51.6% of the AODs changed between 0.1 and 0.3. From Figure 5, almost half of the ALPHA standards were smaller than 0.6 in spring and about 58.8% of the standards changed between 0.8 and 1.2 during the summer. More than 77% of the ALPHA standards ranged between 0.8 and 1.4 in autumn and roughly 69% of the standards were bigger than 0.9 in winters.

The reliance of ALPHA on aerosol optical depth was used by [36] and [37] to acquire the aerosol size distribution. [38], establish that the association amid ALPHA and AOD at 501 nm for four seasons at Dunhuang demonstrated a similar reliance of ALPHA on AOD. [39], also premeditated this association at five locations in China: Dunhuang, Yulin, Beijing, Xianghe, Inner-Mongolia and Liaoning. The outcome demonstrated that since the Dunhuang, Yulin, and Inner-Mongolia locations were sited near dust sources, aerosol loading mostly made up of dust particles, and the association between ALPHA and AOD may well be typified by an incorporated exponential function. The BJ, XH and LN locations demonstrated a more intricate scenario, particularly at the BJ and LN locations. Figure 6 illustrated the disperse plots of immediate ALPHA as a purpose of AOD at 500 nm for each season in Yinchuan. An exponential reliance of ALPHA on AOD in spring is recommended, which is analogous to results detailed by [38] for the Dunhuang, location and for the Dunhuang, Yulin and Inner-Mongolia locations [39]. There is no clear association between ALPHA and AOD for the other seasons, this behavior was also observed by [39] for the BJ and LN locations. And this can be elucidated by the predominance of dust particles with bigger size and aerosol basis is comparatively singleness in spring, and the joint donation of dust and pollutant particles with diverse rate of different aerosol loading and the aerosol basis

is relative intricacy in other seasons. It specified that the main sources of aerosol in Yinchuan changed with diverse seasons. [39], noted out that this distinction of the association between ALPHA and AOD may offer a possible way to recognize and approximate the effects of diverse sources on aerosol loading and aerosol size.

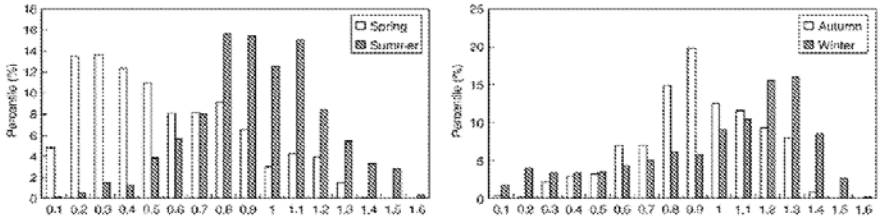

ALPHA (400-675nm) ALPHA (400-675nm)

Figure 5: The frequency distributions of ALPHA 400-675 nm for each season in Yinchuan left: spring and summer; right: autumn and winter (courtesy Atoms)

4.2. Aerosol size circulation

The association amid aerosol size distribution and AOD is imperative for studying aerosol climate forcing. The aerosol size distribution was strong-minded with 21 radius size vats between 11^{-6} cm-2 x 10^{-3} cm. For every month, the average radius of aerosol particles in every vat was computed.

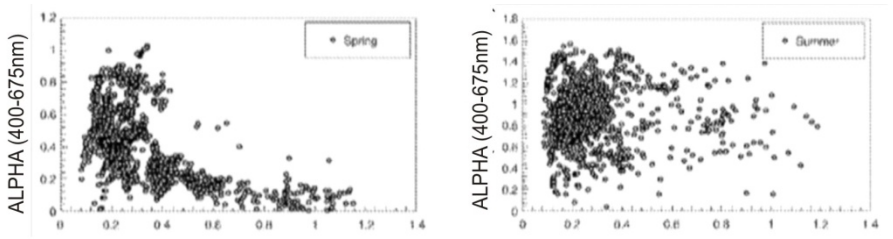

AOD (500nm) AOD (500nm)

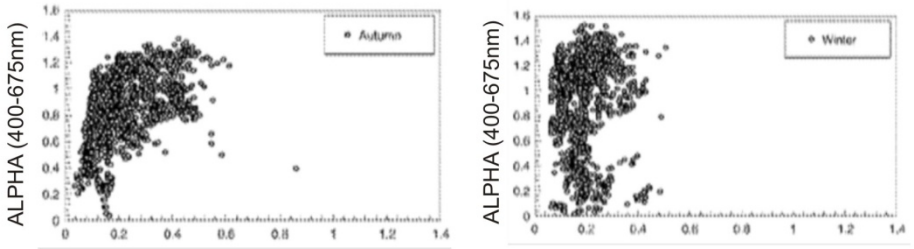

AOD (500nm) (AOD 500nm)

Figure 6: The scatter plots of immediate ALPHA as a role of AOT at 500 nm for each season.(courtesy Atmos)

Figure 7 demonstrated the monthly distinction in aerosol size. The aerosol size distribution has a two-mode formation, which can be typified by the sum of two log-normal distributions as follows:

$$v\,(r) = \frac{dV\,(r)}{d\,\ln r} = \sum_{i=I}^{2} \frac{Kvi}{\sqrt{2\pi}\alpha i} \exp\left[- \frac{(\ln r - \ln r_{v,i})}{\alpha_i^2} \right]$$

Where ɾv,i is the size middle radius, αi is the standard deviation, and Kv,i is the size concentration for accretion and coarse modes. These incorporated quantities can be estimated according to [40]. There is one accretion mode with a radius about 0.16 µm that illustrated a constant monthly difference and a maximum worth in August; this is mostly related to anthropogenic and meteorological circumstances. A coarse mode with a radius of about 8µm is manifest, as are the huge distinction over the months; this mirrors the authority of dust events. There was little modification in the particle volume median radius throughout dust and non dust periods, only revolutionize in particle attention. During the dust incident, the uncouth particle concentration in the atmosphere was about 2-4 times more than that throughout periods when there was no dust motion. The average volume spectrum of huge particles explained as particles with radii larger than

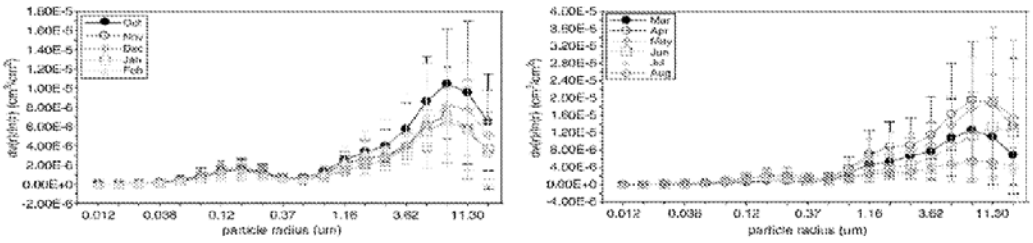

Figure 7: Monthly average of aerosol volume spectrum (500nm) at 21 different radiuses and standard deviation (left; Oct-Feb., right; Mar.-Aug.)(courtesy Atmos).

0.6µm was computed and is equal to 6.04 x 10-7 cm^3/cm^2; for lesser particles the average volume spectrum is 6.58 x $10^{-7} cm^3/cm^2$. The previous is about 10 times greater than the latter, which shows that the uncouth particle concentration was high during the year over the Yinchuan region.

The number of particles in the accretion mode was larger in August than in April and conversely for the coarse mode. Prearranged that the mean AOD standards for these two months are alike, the extinction potential of the accretion mode aerosol was more than that of the uncouth mode aerosol [41].

4.3. Refractive index

The utmost information concerning the refractive index appears from aureole radiances, which are sturdily influenced by errors in the angle-pointing predisposition. And some studies cautiously discussed the refractive index resolved of atmospheric aerosol particles by ground-based solar annihilation and dispersion measurements

[42,17]. The errors are projected to be ± 0.05 in the real fractions of the refractive index and 51% in the imaginary fractions of the refractive index. Figure 8 demonstrates the monthly average of the actual parts of the aerosol refraction index at 400, 500, 675, 870 and 1020 nm. There is no significant distinction of the actual fractions of the refractive index at the diverse wavelengths. This low consideration to wavelengths different faintly with time, but no lucid pattern was found, the average value of the actual part of the refractive index at the 3 highest wavelengths 675, 870, and 1020 nm is 1.5289 as the average value at the 2 lower wavelengths 400 and 500 nm is 1.5100.

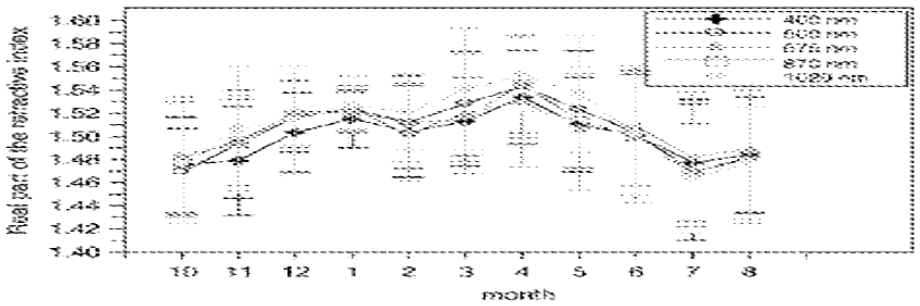

Figure 8: Monthly average definite part of aerosol complex refraction index and standard deviation (courtesy Atmos)

This may be as a result to the emergence of huge amounts of uncouth particles, consequential in a comparatively higher absorption in the near infrared than in the visible [43]. Within the study period, the monthly averaged real fraction of the refractive index arrayed from 1.48 to 1.56 with a mean worth of 1.52. It means that the actual part of the refractive index of dust aerosols is larger than that of anthropogenic aerosols and that the greatest standards emerge in spring, the influence of dust actions over this region throughout this season is obvious.

Figure 9 illustrates the monthly averaged unreal parts of the aerosol refraction index at 5 wavelengths. Comparable to the real parts of the refractive index, the imaginary parts also illustrate a low consideration to wavelength. These results are dependable with the calculated standards of the imaginary parts of the refractive index established in the literatures [43,39]. This low consideration of the unreal parts of the refractive index to wavelength also changed slightly with time. The largest standards of the unreal part of the refractive index are established at 400 nm. The imaginary parts of the refractive index lessened slightly amid 400 and 675 nm and then increased a bit further amid 675 and l020 nm. The average standards of the imaginary fractions of the refractive index at every wavelength were 0.0109, 0.0096, 0.0080, 0.0088 and 0.0099 at 400, 500, 675, 870 and 1020μm, respectively.

The momentous seasonal distinction of the unreal part of the refractive index shows the influence of (courtesy Atmos)different aerosol elements within the Yinchuan area. The biggest average worth of the imaginary part of the refractive index 0.017 emerges in winter, whereas the minimum average value 0.003 is seen throughout the spring. The exceeding results stipulated that dust actions may influence aerosol radiative result through the input of huge amount of dust aerosols, and also through their results on aerosol's bodily and radiative properties.

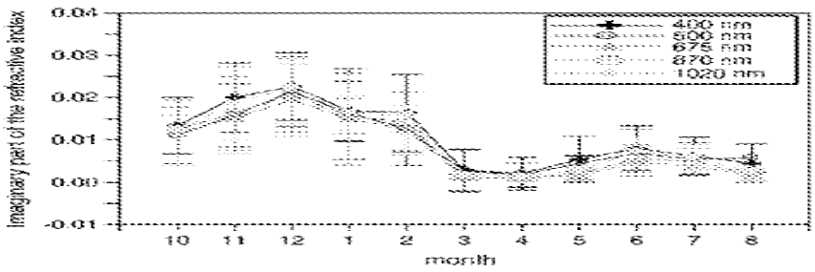

Figure 9: Monthly averaged real imaginary part of aerosol complex refraction index and standard deviation.

4.4. Single dispersion albedo

The single scattering albedo, Φo, is an normal measurement of the relative input of absorption to extinction and is a key changeable in evaluating the climatic effects of aerosols [44,40]. Its importance is typically dependent on the composition substance and size distribution of aerosol particles. The single scattering albedo of desert dust replicated harmony to a number of models [45,46,47,48] ranges from 0.64 to 0.88 at 500 nm, whereas aircraft radiation measurements [49] propose lower absorption Φo 0.96 for the broadband solar spectrum. The major cause of error in the deduced single scattering albedo is owing to standardization of the sky data, and is expected to be ± 0.04.

Table I illustrates the monthly average single dispersion albedo and matching standard deviations at 400, 500, 675, 870 and 1020um. Due to the precision of inversion is lessening with low AOD, only data matching to AOD bigger than 0.4 have been used to statistic. In spring, due to the control of dust events, the scattering input of uncouth particles was enlarged, and the single scattering albedo demonstrated a slight escalating tendency with wavelength [40,20,50]. The single scattering albedo in spring was greatly advanced than that in other seasons, by an average value of 0.95 ± 0.03 at 500 nm. This is lesser than single Scattering albedo standards acquired by others for desert dust 0.95-0.99 [40][51] which hint the probable combination of dust, urban, manufacturing particles and biomass burning aerosols in Yinchuan region. In other periods, the single dispersion albedo reduced with wavelength. However contrast with other studies, this tendency was not theatrical approximately decreased 0.5 from 400 nm to 1020 nm. [52], once established that in air masses within Europe and the Mediterranean, the single scattering albedo reduced piercingly with wavelength from 0.91±0.03 at 440 nm to 0.83 ±0.05 at 1020 nm. So the difference of single scattering albedo with wavelength has provincial characteristics.

4.5. Aerosol scattering Radiative Forcing

The imperative aerosol optical properties and aerosol load may create a considerable impact on aerosols' radiative forcing (ARF) and considerably modify the radiative balance over the area. In our study, the direct radiative forcing effectiveness at surface and TOA at the shortwave array were projected using the SB-DART model. Table 2 demonstrates the aerosol direct radiative forcing effectiveness for each season within Yinchuan region. In spring, the aerosol direct radiative forcing effectiveness significance at surface; TOA is lesser; higher than that in other periods, and these consequences are akin to the calculated standards of the aerosol's direct

radiative forcing effectiveness established in the literatures [20,53]. The cause is mostly due to the control of Asian dust actions in spring, the grid radiation at surface enlarge and the arrival to the top of the atmosphere of radiation also improved. Therefore, the atmospheric radiation absorption rate reduced. And the direct radiative forcing competence worth at the shortwave range is-55.32,-59.72,-60.14 and-60.39 at surface and 13.90, 10.40, 2.31 and 2.65 at TOA in spring, summer, autumn and winter, in that orderly.

Table 1: Monthly averaged single scattering albedo with corresponding standard deviations

	400nm	500nm	675nm	870nm	1020nm	
Oct	0.89±0.03	0.87±0.02	0.87±0.03	0.85±0.03	0.85±0.04	
Nov	0.87±0.02	0.87±0.03	0.85±0.03	0.84±0.03	0.83±0.04	
Dec	0.85±0.02	0.83±0.03	0.83±0.03	0.82±0.04	0.80±0.03	
Jan	0.85±0.02	0.84±0.02	0.83±0.03	0.82±0.02	0.81±0.04	
Feb	0.87±0.02	0.84±0.02	0.85±0.02	0.85±0.03	0.86±0.03	
Mar	0.93±0.03	0.95±0.03	0.95±0.03	0.96±0.02	0.98±0.03	
Apr	0.91±0.03	0.92±0.03	0.93±0.03	0.95±0.03	0.96±0.03	
May	0.92±0.03	0.95±0.03	0.95±0.03	0.96±0.03	0.97±0.04	
Jun	0.91±0.03	0.91±0.03	0.88±0.03	0.88±0.04	0.90±0.04	
Jul	0.89±0.03	0.87±0.03	0.85±0.03	0.85±0.03	0.83±0.03	
Aug	0.89±0.02	0.86±0.02	0.85±0.03	0.84±0.02	0.83±0.03	

Table 2: Aerosol direct radiative forcing effectiveness for each session

	Spring	**Summer**	**Autumn**	**Winter**
Surface (W. m^{-2})	-055.32	-59.72	-60.14	-60.39
TOA (W. m^{-2})	13.80	10.40	2.31	2.65

5. Summaries and Conclusion

Aerosol optical depth (AOD), Angstrom wavelength exponent (ALPHA), amount size distributions, refraction index and single scattering albedo within Yinchuan, a town in northwest China, were retrieved using the data of sky radiometer from October 2003 to August 2004.

The AOD over the Yinchuan region differ with season, with a vernal utmost and a winter lowest least, and is mostly influenced by weather circumstances, dust events and anthropogenic. The greatness of ALPHA was comparatively high all through the year, signifying the greater input of fine particles to extermination in the area; the highest standards were seen in winter and the least standards emerge in spring. The diurnal inconsistency of AOD in Yinchuan changed about 32%, 34%, 25% and 39% in spring, summer, autumn and

winter, in that order, and demonstrated a similar distinction pattern in spring, summer and autumn and had another difference pattern in winter. The frequency circulation of AOD and ALPHA roughly follows a log-usual circulation and a usual probability circulation, respectively. In the spring, approximately 82% of the AODs ranged amid 0.1 and 0.6 and 56% of the AOD ranged amid 0.4 and 0.6; about 73%, 67% and 80.9% varied between 0.1 and 0.4 in summer, autumn and winter, respectively. The greatness of nearly half of the ALPHA standards were smaller than 0.6 in spring and about 58.8% of the standards ranged amid 0.8 and 1.4 in summer; in autumn and winter, about 77% of the standards varied between 0.8 and 1.4 and roughly 69% of the standards were larger than 0.9, in that order. The association between ALPHA and AOD demonstrate a simple reliance of ALPHA on AOD in spring and can be typify by one incorporated exponential function. No obvious reliance of ALPHA on AOD was apparent in other seasons, signifying that the major foundation of aerosol in Yinchuan changed with season.

The aerosol amount size distribution can be typify by the sum of two log-usual circulations, and has two modes: an accretion mode with a radius of 0.16μm utmost in August, and a loutish mode with a radius of 8 μm utmost in April and May.

The actual and the unreal parts of the refraction index are evidently affected by dust actions, with the real parts growing in spring and the imaginary parts lessening in spring. Both actual and unreal parts of the refractive index are not sensitive to wavelength though a trivial distinction with time was observed. The actual fraction of the refractive index were commonly advanced at the near-infrared wavelengths average value is 1.5289 than at the visible wavelengths average value = 1.5100. The magnitude unreal part of the refractive index reduced slightly amid 400 and 675 nm and then increased amid 675 and 1020 nm.

The single scattering albedo in spring was plainly higher than in other seasons and demonstrated a slight rising tendency with wavelength. In other season, the single scattering albedo reduced with wavelength. The distinction of single scattering albedo with wavelength has area characteristics, which is substantiated by other studies. The single scattering albedo standards acquired in spring are lower than those detailed by others for desert dust 0.96-099, which proposes the likely mixture of dust, city, manufacturing particles and biomass burning aerosols within Yinchuan. Concerning the aerosol radiative effects within Yinchuan region, the aerosol direct radiative forcing effectiveness assessment at surface; TOA in spring is lower and higher than in other period. The importance of it is -55.32, -59.72, -60.14 and -60.39 at surface and 13.90, 10.40, 2.31 and 2.65 at TOA in spring; summer, autumn and winter, in that orderly.

6. Recommendation

A second-derivative smoothing method, universally used in inversion work, is applied to the quandary of inferring total columnar ozone magnitude and aerosol optical depths. The application is exceptional in that the anonymous may be solved for directly without utilizing standard inversion methods. It is shown, though, that by utilizing inversion constraints, better solutions are usually obtained. The technique is quite versatile and able to deal with anecdotal total ozone and various aerosol size distributions.

This paper progress the study of the link between $PM_{2.5}$ and meteorological stricture for the purpose of epidemiological studies. Nevertheless, the quandary is complex and necessitates more attention in the future.

7. Repudiation

This is an edition of not adapted manuscript that has been accepted for publication. As a service to authors and researchers we are on condition that this version of the accepted manuscript "a.m". Copyediting, typesetting, and appraisal of the resulting proof will be undertaken on this manuscript prior to final publication of the edition of record "e.o.r". For the duration of production and pre-press, errors may be revealed which may affect the content, and all legal disclaimers that be-relevant to the journal relate to this edition also.

Acknowledgments

We thank Prof. Guangyu Shi, Institute of Atmospheric Physics, Chinese Academy of Sciences, for providing the direct and scattering solar irradiance data from Yinchuan for this study. We are grateful to the Open CLASTR project for use of their 'SKYRAD' parcel in this study. We also express appreciation Maki Yamano, Center for Climate System Research, University of Tokyo, for her help in the management of the code

Reference

[1]. Mao, J., Li, C., 2006. Observation study of aerosol radiative properties over China. Acta Meteorlogica Sinica 20 (3), 306-321.

[2]. Xin, J., Wang, Y., Li, Z., Wang, P., Hao, W., Nordgern, B., et al. AOD and Angstrom parameters of aerosols observed by the Chinese sun hazemeter Network from August to December 2004. Journal of Geophysical Research 112, D05203. doi:I0.1029!2006JD007075.

[3]. Wang, H., Shi, G., Aeruo, A., Wang, B., Zhang, T., 2004. Radiative forcing due to dust aerosol over east Asia-north Pacific region during spring, 2001. Chinese Science Bulletin 49(20), 2212-2219.

[4]. Chen, Y, Lohmann, U., Zhang, J., Luo, Y., Liu, Z., Lesins, G., 2005. Contribution of changes in sea surface temperature and aerosol loading to the decreasing precipitation trend in Southern China. Journal of Climate 18 (9), 1381-1390.

[5]. Kaufman, Y.J., Tanre, D., Boucher, O., 2002. A satellite view of aerosols in the climate system. Nature 419, 2 15-223.

[6]. Dubovik, O., Holben, B., Eck, T. F., Smirnov, A., Kaufman, Y.J., et al., 2002. Variability of absorption and optical properties of key aerosol types observed in worldwide locations. Journal of the Atmospheric Sciences 59, 590-608.

[7]. Osborne, S. R., Haywood, J. M., Francis, P. N., Dubovik, O., 2004. Short-wave radiative effects of biomass burning aerosol during SAFARI2000. Q.J.R. Meteorology Society 130, 1423-1448.

[8]. Bates, T.S., Anderson, T. l., Baynard, T., Bond, T., Boucher, 0., Carmichael, G., et al., 2006. Aerosol direct radiative effects over the northwest Atlantic, northwest Pacific, and North Indian Oceans: estimates based on in situ chemical and optical measurements and chemical transport modeling. Atmospheric chemistry Physical Discussion 6, 175-362.

[9]. Kelly, J.T., Chuang, C.C., Wexler, AS., 2007. Influence of dust composition on cloud droplet formation. Atmospheric Environ- ment 41, 2904-2916.

[10]. IPCC, 2001. Climate change 2001. The Scientific Basis-Contribution of Working Group I to the third Assessment Report of the Intergovernmental Panel on Climate Change. Cambridge University Press, New York.

[11]. IPCC, 2007. Climate change 2001 the scientific basis. In: Solomon, S., Qin, D., Manning, M., et al. (Eds.), Contribution of Working Group I to the Forth Assessment Report of the Intergovernmental Panel on Climate Change. Cambridge University Press, Cambridge, United Kingdom and New York, NY, USA.

[12]. Hansen, J., Sato, M., Ruedy, R., Lacis, A., Oinas, V., 2000. Global warming in the twenty-first century: an alternative scenario. Proceedings of the National Academy of Sciences of the United States of America 97, 9875-9880.

[13]. Holben, B.N., Kaufman, Y.J., Eck, T.F., Slutsker, I., Tame, D., et al., 1998. AERONET—a federated instrument network and data archive for aerosol characterization. Remote Sensing of Environment 66, 1-16.

[14]. Holben, B.N., Tame, D., Smirnov, A., Eck, T.F., Slutsker, I., Abuhassan, N., et aL, 2001. An emerging ground-based aerosol climatology: aerosol optical depth from AERONET. Journal of Geophysical Research 106, 12,067-12,097.

[15]. Takamura, T., Nakajima, T., Okada, I., Uchiyama, A., Sugimoto, N., Shi, G., et al. Aerosol Cloud-radiation Study Using the SKYNET Data. The first ADEC Workshop, Tokyo, Japan. http:!/ www.aeoliandust.com.

[16]. WMO, 2001. Strategy for the implementation of the global atmosphere watch programme (2001-2007). WMO No. 142. World Meteorological Organization, Geneva, pp. 43-45.

[17]. Tonna, G., Rao, R., Nakajima, T., 1995. Aerosol features retrieved from solar aureole data: a simulation study concerning a turbid atmosphere. Applied Optics 34, 4486-4499.

[18]. Schmid, B., Spyak, P.R., Biggar, S.F., Wehrli, C., Sekler, J., Ingold, T., et al., 1998. Evaluation of the applicability of solar and lamp radiornetric calibrations of a precision sun photometer operating between 300 andlO25 nm. Applied Optics 37, 3923-3941.

[19]. Tanaka, M., Nakajima, T., Shiobara, M., 1986. Calibration of a sunphotometer by simultaneous measurements of direct-solar and circumsolar radiations. Applied Optics 25, 1170-1176.

[20]. O'Neill, NT., Miller, JR., 1984. Combined solar aureole and solar beam extinction measurements. I: calibration considerations. Applied Optics 23, 369 1-3696.

[21]. Nakajima, T., Tonna, T., Rao, R., Boi, P., Kaufman,Y.J., Holben, B., 1996. Use of sky brightness measurements from ground for remote sensing of particulate polydispersions. Applied Optics 35, 2672-2686.

[22]. Tonna, G., Rao, R., Nakajima, T., 1995. Aerosol features retrieved from solar aureole data: a simulation study concerning a turbid atmosphere. Applied Optics 34, 4486-4499.

[23]. Smirnov, A., Holben, B.N., Eck, T.F., Dubovik, O., Slutsker, I., 2000. Cloud screening and quality control algorithms for the AERONET data base. Remote Sensing of Environment 73, 337-349.

[24]. Xia, X., Wang, P., Chen, H., Gouloub, P., Zhang, W., 2005. Ground- based remote sensing of aerosol optical properties over north China in spring. Journal of Remote Sensing 9 (4), 429-437.

[25]. Ricchiazzi, P., Yang, SR., Gautier, C., Sowle, D., 1998. SBDART: a research and teaching software tool for plane-parallel radiative transfer in the Earth's atmosphere. Bulletin of the American Meteorological Society 79 (10), 2101-2114.

[26]. Stamnes, K., Tsay, S.C., Wiscombe, W., Jayaweera, K., 1988. Numerically stable algorithm for discrete-ordinate-method radiative-transfer in multiple-scattering and emitting layered media. Applied Optics 27 (12), 2502-2509.

[27]. Lyamani, H., Olmo, F.J., Alcantara, A., Alados-Arboledas, L., 2006a. Atmospheric aerosols during the 2003 heat wave in southeastern Spain I: spectral optical depth. Atmospheric Environment 40, 6453-6464.

[28]. Liu, Y., Niu, S., Zheng, Y., 2004. Optical depth characteristics of Yinchuan atmospheric aerosols based on the CE-3 1 8 sun tracking spectrophotometer data. Journal of Nanjing Institute of Meteorology 27 (5), 6 15-622.

[29]. Kaufman, Y.J., Tanre, D., Dubovik, 0., Karnieli, A., Remer, L.A., 2001. Absorption ofsunlight by dust as inferred from satellite and ground-basedremote sensing. Geophysical Research Letters 28 (8), 1479-1482.

[30]. Smirnov, A., Holben, B.N., Eck, T.F., Slutsker, I., Chatenet, B., Pinker, R.T., 2002. Diurnal variability of aerosol optical depth observed at AERONET (Aerosol Robotic Network) sites. Geophysical Research Letters 29 (23), 2115. doi:IO.1029/2002GL016305.

[31]. Peterson, J.T., Flowers, E.C., Beth, G.J., Reynolds, C.L., Rudisill, J.H., 1981. Atmospheric turbidity

over central North Carolina. Journal of Applied Metalworking 20, 229-241.

[32]. Xia, X., Chen, H., Wang, P., Zhang, W., Goloub, P., Chatenet, B., et al. Variation of column-integrated aerosol properties in a Chinese urban region. Journal of Geophysical Research 111, D05204. doi:IO.1029!2005JD006203.

[33]. O'Neill, N.T., Ignatov, A., Holben, B.N., Eck, T.F., 2000. The lognonnal distribution as a reference for reporting aerosol optical depth statistics; empirical tests using multi-year, multi-site AERONET sunphotometer data. Geophys. Res. Lett. 27(20), 3333-3336.

[34]. Matthias, V., Bosenberg, J., 2002. Aerosol climatology for the planetary boundary layer derived from regular lidar measurements. Atmos. Res. 63, 221-245.

[35]. Nwofor, O.K., Chidiezie Chineke, T., Pinker, R.T., 2007. Seasonal characteristics of spectral aerosol optical properties at a subSaharan site. Atmospheric Chemistry 85 (1), 38-51.

[36]. Fouquart, Y., Bonnel, B., Brgniez, J.C., et al, 1987. Observation of Saharan aerosols: results of ECLATS Field experiment: IL Broadband radiative characteristics of the aerosols and vertical radiative flux divergence. Journal of climate and Meteorology 25, 38-52.

[37]. D'almeida, GA., 1987. On the variability of desert aerosol radiative characteristics. Journal of Geophysical Research 92, 3017-3026.

[38]. Xia, X., Chen, H., Wang, P., 2004. Aerosol properties in a Chinese semiarid region. Atmospheric Environment 38, 4571-4581.

[39]. Xia, X., Wang, P., Chen, H., Gouloub, P., Zhang, W., 2005. Ground- based remote sensing of aerosol optical properties over north China in spring. Journal of Remote Sensing 9 (4), 429-437.

[40]. Zhang, W., Hu, B., Chen, C., Du, P., Zhang, L., Feng, G., 2004. Scattering properties of atmospheric aerosols over Lanzhou City and applications using an integrating nephelometer. Advances in Atmospheric Science 21(6), 848-856.

[41]. Wendisch, M., Hoyningen-Huene, W., 1994. Possibility of refractive index determination of atmospheric aerosol particles by ground- based solar extinction and scattering measurements. Atmospheric Environment 28 (5), 785-792.

[42]. Yu, X., Cheng, T., Chen, J., Liu, Y., 2006. A comparison of dust properties between China continent and Korea, Japan in East Asia. Atmospheric Environment 40, 5787-5797.

[43]. Cheng, T., Wang, H., Xu, Y., Li, H., Tian, L., 2006a. Climatology of aerosol optical properties in northern China. Atmospheric Environment 40, 1495-1509.

[44]. Cheng, T., Liu, Y., Lu, D., Xu, Y., Li, H., 2006b. Aerosol properties and radiative forcing in Hunshan Dake desert, northern China. Atmospheric Environment 40, 2169-2179.

[45]. Jacobson, M.Z., 2000. A physically-based treatment of elemental carbon optics: implications for global direct forcing of aerosols. Geophysical Research Letter 27, 2 17-220.

[46]. Shettle, E.P., Fenn, R.W., 1979. Models of aerosols of lower troposphere and the effect of humidity variations on their optical proprieties. AFCRL Tech. Rep. 79 0214. Air Force Cambridge Research Laboratory, Hanscom Air Force Base, MA, p. 100.

[47]. WMO, 1983. Radiation commission of JAPAM meeting of experts on aerosol and their climatic effects. World Meteorological Organisation Rep. WCP55, 28-30.

[48]. Koepke, P., Hess, M., Schult, I., et al., 1997. Global aerosol data set. MPI Meteorologic Hamburg Rep., 243, p. 44.

[49]. Hess, M., Koepke, P., Schult, I., 1998. Optical properties of aerosol and clouds: the sofiware package OPAC, Bulletin of the American Meteorological Society 79, 831-844.

[50]. Lyamani, H., Olmo, F..J., Alcantara, A., Alados-Arboledas, L., 2006b. Atmospheric aerosols during the 2003 heat wave in southeastern Spain II: microphysical columnar properties and radiative forcing. Atmospheric Environment 40, 6465-6476.

[51]. Prasad, A . K., et al., 2007. Aerosol radiative forcing over the IndoGangetic plains during major dust storms. Atmospheric Environment. doi:10.10161j.atmosenv.2007.03.060.